A Shock Grammar For Recognition

Kaleem Siddiqi

Department of Electrical Engineering
McGill University
Montreal, Canada H3A 1Y2

Benjamin B. Kimia

Division of Engineering
Brown University
Providence, RI 02912

Abstract

We confront the theoretical and practical difficulties of computing a representation for two-dimensional shape, based on **shocks** *or singularities that arise as the shape's boundary is deformed. First, we develop subpixel* **local** *detectors for finding and classifying shocks. Second, we show that shock patterns are not arbitrary but obey the rules of a grammar, and in addition satisfy specific topological and geometric constraints. Shock hypotheses that violate the grammar or are topologically or geometrically invalid are pruned to enforce* **global** *consistency. Survivors are organized into a hierarchical graph of shock groups computed in the reaction-diffusion space, where diffusion plays a role of regularization to determine the significance of each shock group. The shock groups can be functionally related to the object's* **parts, protrusions** *and* **bends**, *and the representation is suited to recognition: several examples illustrate its stability with rotations, scale changes, occlusion and movement of parts, even at very low resolutions.*

1 Introduction

What does it mean to *recognize* an object from its shape? Informally, this implies an identification of the shape with a familiar category or class of objects, Figure 1. This notion of categorization is crucial to many vision tasks, such as searching a database of shapes rapidly, reasoning about the attributes of new or unfamiliar shapes, *etc.* Curiously, whereas this ability to categorize appears to come naturally and effortlessly to humans, it has been extremely difficult to formalize for computers. In this paper, we address the computational aspects of this problem; specifically, we investigate the description of generic shape classes from the mathematical perspective of curve evolution.

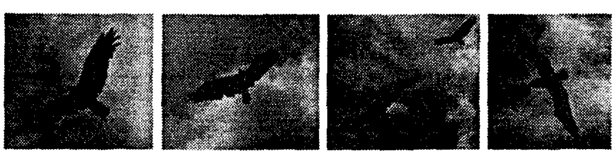

Figure 1: These birds are effortlessly grouped into two categories, based on similarity in "form".

Existing proposals for shape representation emphasize properties of its region, *e.g.*, symmetry and thickness [1], or of its boundary, *e.g.*, curvature extrema [20] and inflection points, or of both [2]. An alternate classification is according to those where shape is viewed statically as a combination of *primitives*, *e.g.*, generalized cylinders, versus those where shape is explained developmentally via a set of processes acting on a simpler shape [14]. Returning to the region-based *symmetric axis transform* (SAT) [1], this view has spawned a vast literature on the theoretical and computational aspects of skeletons. However, it is unfortunate that Blum's key insight that the SAT provides for qualitative shape descriptions in terms of "shape morphemes", *e.g.*, disc, worm, wedge, flare, *etc.*, is usually forgotten. Curiously, an evolutionary approach to shape description supports and complements this view, and gives it a sound mathematical foundation [8, 10]. To elaborate, Kimia *et al.* explore deformations of the shape's boundary, a special case of which is deformation by a linear function of curvature κ:

$$\boxed{\begin{cases} \frac{\partial \mathcal{C}}{\partial t} & = (\beta_0 - \beta_1 \kappa)\vec{N} \\ \mathcal{C}(s,0) & = \mathcal{C}_0(s). \end{cases}} \qquad (1)$$

Here $\mathcal{C}$ is the boundary vector of coordinates, $\vec{N}$ is the outward normal, s is the path parameter, t is the time duration (magnitude) of the deformation, and β_0, β_1 are constants. The space of all such deformations is spanned by the ratio β_0/β_1 and time t, constituting the two axes of the *reaction-diffusion space.* Underlying the representation of shape in this space are a set of *shocks* [11], or entropy-satisfying singularities, which develop during the evolution and are classified into four types, Figure 2 (left): 1) A FIRST-ORDER SHOCK is a discontinuity in orientation of the shape's boundary; 2) A SECOND-ORDER SHOCK is formed when two distinct non-neighboring boundary points collide, but none of their immediate neighbors collapse together; 3) A THIRD-ORDER SHOCK is formed when two distinct non-neighboring boundary points collide, such that the neighboring boundary points also collapse together[1]; and 4) A FOURTH-ORDER SHOCK is formed when a closed boundary collapses onto a single

[1] Whereas third-order shocks are not generic they merit a distinct classification because of their psychophysical relevance [9] and the abundance of biological and man-made objects with "bend-

1063-6919/96 $5.00 © 1996 IEEE

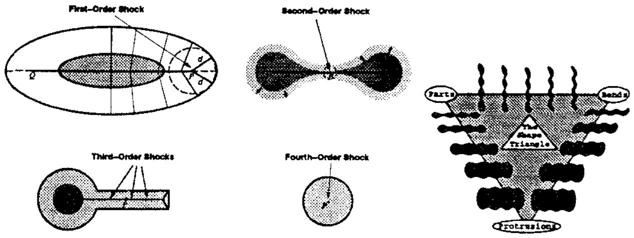

Figure 2: LEFT: The four shock types. RIGHT: The sides of the shape triangle represent continua of shapes; the extremes correspond to the "parts", "bends" and "protrusions" nodes [9].

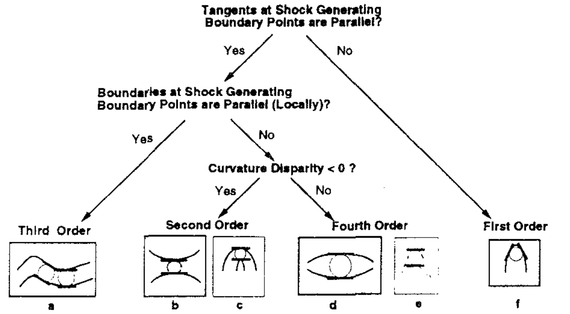

Figure 3: A classification of shock types based on the tangents and the local neighborhood of the two shock generating boundary points. The curvature disparity is the sum of the two (signed) curvatures.

point. While these definitions are intuitive, they do not easily lend themselves to algorithms for shock detection. A key idea of this paper is that shock computations can be made robust by relying not only on better (subpixel) *local* detectors and classifiers, but also on *global* interactions between shocks, through a shock grammar. In related work, Leymarie and Levine have simulated the grassfire transform using active contours [13]; Scott *et al.* have suggested the use of wave propagation to obtain the full symmetry set [21]; Kelly and Levine have demonstrated the use of annular operators in obtaining coarse object descriptions from real imagery [7]; and Pizer *et al.* have proposed a computational model for object representation via "cores", or regions of high medialness in intensity images [2]. Our work extends the above approaches in a number of ways, which are perhaps best understood in the context of the distinction between shocks and skeletons.

The set of shocks which form along the reaction axis reduces to the traditional skeleton when information regarding *type*, *group*, and *salience* is discarded [23]. However, first, the notion of *type* is essential to capture *qualitative* aspects of shape, leading to generic perceptual shape classes[2] and algorithms for obtaining them, Section 2. Second, the *grouping* of shocks depends not only on their type but also on *sequential*, *geometric* and *topological* constraints obtained from a history of shocks, Section 3. This results in a *hierarchical* representation of shape by shock groups, as illustrated by numerous examples, Section 4. Third, the notion of *salience* connects "nearby" shapes, *e.g.*, Figure 19, providing a foundation for a topology over shape for recognition. In conclusion, we suggest how the shock-based framework might be extended to apply directly to images, Section 6.

like" components, *e.g.*, fingers, limbs, legs of a table, *etc.* Also, they are simultaneously the limit of first-order shocks travelling with infinite speed, but in opposite directions.

[2]First-order shock groups describe "protrusions", second-order shocks occur at "necks", third-order shock groups describe "bends", and viewing the evolution in reverse, fourth-order shocks are *seeds* from which the shape is grown [9].

2 Shock Classification and Detection: Local Operators

In the design of shock detection operators we face two primary challenges: that of arriving at a complete shock classification scheme which leads to a computational algorithm for detection, and that of obtaining accurate geometric estimates without blurring across singularities. We discuss shock classification and detection in turn.

2.1 Classification of Shocks

An intuitive approach is to classify a shock based on properties of the boundary points which collide at it, Figure 3. Whereas this classification provides insight it is difficult to implement directly, *e.g.*, the mapping of a shock to its associated bi-tangent points can become intractable in the presence of multiple nearby topological splits. Alternatively, one may rely on the differential properties of an *embedding surface*, an approach which proves to be computationally efficient and robust. For theoretical as well as numerical reasons, the original curve flow is embedded in the level set evolution of an evolving surface [3, 17], $z = \phi(x, y, t)$:

$$\phi_t + \beta(\kappa)|\nabla\phi| = 0, \qquad (2)$$

with the correspondence that the evolving shape is represented at all times by its zero level set $\phi(x, y, t) = 0$. For convenience we take the initial surface ϕ_0 to be the signed distance function to the shape's boundary (although any Lipshitz continuous function will suffice [3]). The classification of shocks based on differential properties of ϕ is summarized in Figure 4 and Table 1. A **first-order** shock corresponds to a discontinuity in the orientation of the tangent $\vec{T}$ to the level curve, computed from ϕ as $\arctan(\frac{-\partial\phi/\partial x}{\partial\phi/\partial y})$. Since the colliding boundary points have normals pointing in opposite directions, $|\nabla\phi| = 0$ at **second-**,**third-** and **fourth-order** shocks. These shocks can be distinguished from one another by the Gaussian curvature, Table 1. Note that this classification is invariant to the choice of the embedding surface and that all

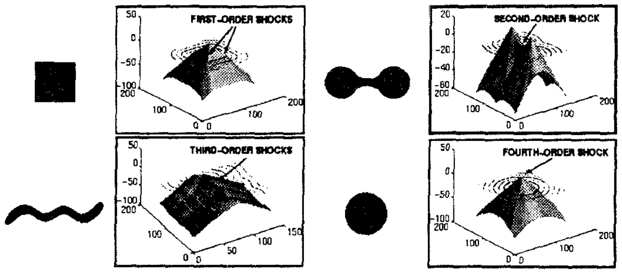

Figure 4: Shock classification based on properties of an embedding surface. TOP LEFT: First-order shocks occur at corners, corresponding to creases on the surface with $|\nabla\phi| > 0$. TOP RIGHT: A second-order shock corresponds to a hyperbolic point with $|\nabla\phi| = 0$. BOTTOM LEFT: Third-order shocks correspond to parabolic points with $|\nabla\phi| = 0$. BOTTOM RIGHT: A fourth-order shock corresponds to an elliptic point with $|\nabla\phi| = 0$.

Shock Type	Orientation	Curvature
First	non-vanishing $\nabla\phi$	high κ
Second	isolated vanishing $\nabla\phi$	$\kappa_1\kappa_2 < 0$
Third	non-isolated vanishing $\nabla\phi$	$\kappa_1\kappa_2 = 0$
Fourth	isolated vanishing $\nabla\phi$	$\kappa_1\kappa_2 > 0$

Table 1: Shock classification based on the gradient $|\nabla\phi|$, the level set curvature κ, and the principal curvatures κ_1, κ_2 of the surface.

the necessary quantities can be computed locally[3].

2.2 Subpixel Shock Detection

We develop a subpixel implementation of the above ideas in order to obtain accurate geometric estimates in the vicinity of discontinuities and to localize shocks. Note that whereas the level set formulation supports subpixel curve evolution an algorithm that only attempts to locate shocks at grid points will suffer from discretization artifacts.

A class of techniques called *essentially non-oscillatory* (ENO) schemes have recently been introduced in the numerical analysis literature to address the problem of inaccurate differential estimates in the vicinity of discontinuities [6]. The basic idea is to select between two contiguous sets of data points for interpolation the one which gives the lower variation, such that at regions neighboring a discontinuity the smoothing is always from the side *not* containing it. By replacing polynomials with *geometric* interpolants: lines, circular arcs, *etc.*, these ideas have been adapted to the 2D problem of locating level curves of an embedding surface while preserving and explicitly placing orientation discontinuities (first-order shocks) [24]. The method provides a subpixel contour tracer (for open and closed curves) which can be used to recover the shape's contour from the evolving embedding surface, Figure 5, and can be extended to higher order shock detection as follows. Recall that $|\nabla\phi| = 0$ at higher order shocks. Therefore, the geometric interpolation method may be used to find ϵ crossings of $|\nabla\phi|$, Figure 6 (left). However, this approximation always yields 2D *regions* surrounding the putative shock points. As a solution, since ϕ_x *and* ϕ_y *must each go to zero independently* for $|\nabla\phi|$ to go to zero, the problem can be reduced to two 1D problems by considering zero-crossing curves of ϕ_x and ϕ_y[4], and finding overlaps, Figure 6 (right). This suggests the algorithm for higher order shock detection outlined in Figure 7; further details appear in [23].

[3] $|\nabla\phi| = (\phi_x^2 + \phi_y^2)^{1/2}$; $\kappa_1\kappa_2 = \frac{\phi_{xx}\phi_{yy} - \phi_{xy}^2}{(1+\phi_x^2+\phi_y^2)^2}$; $\kappa_1 + \kappa_2 = \frac{(1+\phi_x^2)\phi_{yy} - 2\phi_x\phi_y\phi_{xy} + (1+\phi_y^2)\phi_{xx}}{(1+\phi_x^2+\phi_y^2)^{3/2}}$.

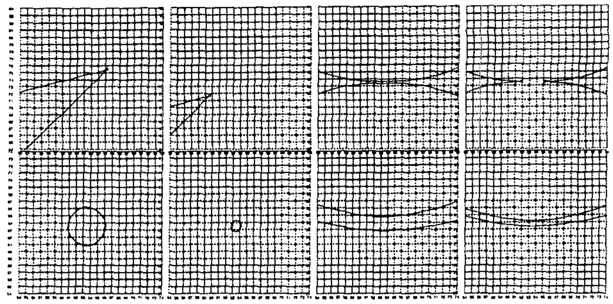

Figure 5: CLOCKWISE FROM TOP LEFT: The *geometric* ENO interpolation technique [24] preserves discontinuities in the vicinity of first- , second-, third-, and fourth-order shocks; gridlines are overlayed and detected corners are marked.

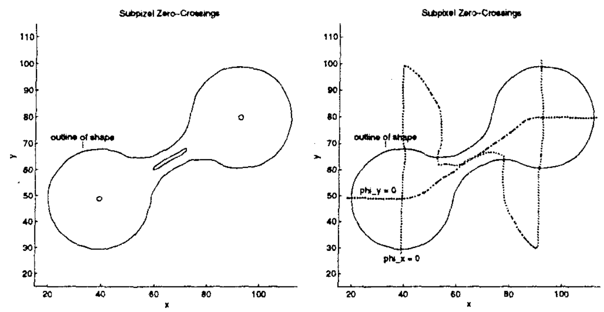

Figure 6: LEFT: The zero crossing contours of $(|\nabla\phi| - \epsilon)$ demarcate regions around the putative shock points. RIGHT: Zero-crossing curves of ϕ_x and ϕ_y intersect at *exactly* three points, two of which are fourth-order shocks, and one of which is a second-order shock, as determined from the sign of $\kappa_1\kappa_2$.

3 Shock Grouping: Global Interactions

The fact that the set of shocks formed under pure reaction ($\beta_1 = 0$) provides the SAT [23] implies that geometric and topological properties that hold for skeletons, *e.g.*, those studied in [4, 22], must hold for shocks as well. We examine three types of constraints on shock formation in Figure 8: *sequential*, *geometric* and *topolog-*

[4] Care must be taken to avoid regions where either ϕ_x or ϕ_y is identically zero over a neighborhood of grid points. Fortunately, ϕ_x and ϕ_y cannot both be identically zero over the same regions, since that would imply a 2D region of third-order shocks, which is an impossibility.

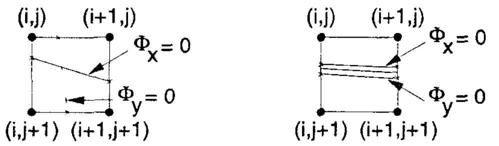

Figure 7: Higher order shock detection based on overlaps of $\phi_x = 0$ and $\phi_y = 0$ within a cell. The four neighboring grid points are marked with filled circles. LEFT: When the two curves pass through the same cell and are not parallel, a second-order or fourth-order shock is placed at the point of intersection (provided that it lies within the cell), based on the sign of the Gaussian curvature. RIGHT: When the two curves pass through the same cell and are close to parallel (their slopes are within 10 degrees), a set of third-order shocks is interpolated as a line drawn through the averaged endpoints.

ical; the first type pertains to allowed sequences of shocks in a group; the latter two relate to properties of one or more shock groups (smoothness, connectivity, *etc*). The constraints suggest a course of actions to be taken in order to prune impossible shock configurations and organize survivors into more global structures, Figure 10. Further, the sequential constraints can be concisely described via a shock grammar. Formally, a *grammar* G is a language generating device, which is defined by a quadruple (V, Σ, R, S) [12]. Here V is an alphabet divided into two parts, the set of *terminal* symbols $\Sigma \subseteq V$ and the set of *non-terminal* symbols $V - \Sigma$. S, the *start* symbol, is an element of $V - \Sigma$ and R, the set of *rules*, is a finite subset of $V^*(V - \Sigma)V^* \times V^*$ The grammar operates by beginning with a start symbol and then constructing a string via repeated applications of the rules, *i.e.*, by identifying a substring in the current string which appears on the left hand side of one of the rules, and replacing it with the string that appears on the right hand side of that rule. We introduce a **shock grammar**, SG, as follows:

$V = \{S_1, S_2, S_{\bar{3}}, S_4, S_I, S_T, E\}$
$\Sigma = \{S_T\}$
$R = \{S_I \to S_1 E, S_I \to S_2 E, S_I \to S_{\bar{3}} E, S_I \to S_4, S_1 E \to S_1 S_1 E, S_1 E \to S_1 S_{\bar{3}} E, S_1 E \to S_4, S_2 E \to S_2 S_1 E, S_{\bar{3}} E \to S_{\bar{3}} S_1 E, S_{\bar{3}} E \to S_{\bar{3}} S_T, S_4 \to S_4 S_T\}$.

The symbols S_1, S_2, S_4 represent first-, second-, and fourth-order shocks. S_I is a start symbol, S_T is a terminal, and since third-order shocks never appear in isolation, a group of third-order shocks is an element of the alphabet, denoted by $S_{\bar{3}}$. E represents the end of a growing shock sequence and is used to enforce the requirement that shocks be added only to that end, making the grammar context dependent. Figure 9 illustrates the application of the grammar. Note that whereas the grammar suffices to describe the composition of a shock group, it does not reflect the geometric and topological constraints; this may be possible by embedding the grammar in a graph.

P1. First order shocks flow with finite speed, except for a set of isolated points (*e.g.*, initial first-order shocks flowing outwards from a second-order shock).
P2. First and third-order shock directions change continuously, *i.e.*, these shock branches cannot have any corners.
P3. Second-order shocks are initial and are isolated from other second-order, third-order, and fourth-order shocks.
R1. Once formed, a second-order shock must give rise to two first-order shocks that flow out of it. The speed of each first-order shock is infinite.
P4. A first-order shock branch can either merge with another first-order shock branch, terminate in a third-order shock branch, or terminate in a fourth-order shock.
P5. Two third-order shock branches cannot intersect.
P6. A first-order branch can flow into or out of a third-order branch's endpoints, but never into or out of a point that lies in the interior of a third-order branch.
R2. A single first-order branch that flows into or out of a third-order branch's endpoints, should maintain continuity of orientation.
P7. Fourth-order shocks are terminal.
P8. A circle is the only shape described by an isolated (fourth-order) shock. Non-circular shapes cannot have any isolated shocks.
R3. For non-circular shapes, each fourth-order shock must have at least one first-order shock branch flowing into it.

Figure 8: Proofs and explanations of propositions **P1-P8** and remarks **R1-R3** appear in [23]. An *initial* shock is one which may give rise to other shocks, but can have no shocks flowing into it; a *terminal* shock has no shocks flowing out of it, but may have shocks flowing into it.

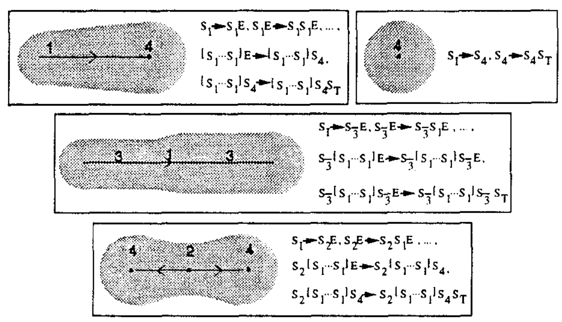

Figure 9: The examples illustrate the construction of different shock groups by repeated application of the rules of the shock grammar.

4 Examples

We illustrate the robustness of our two-stage numerical algorithm for shock detection and classification with several examples. The reconstructions are simulations of the "growth" of each shape from its shock-based representation, with linear interpolation of the radius function between successive shocks on the same branch[5]. Figure 11 depicts the evolution of shocks for a

[5]The initial distance transform is blurred very slightly to combat discretization effects, hence the reconstructions have slightly rounded corners.

A1. A first-order shock should be appended to the end of an existing first-order shock group so long as it: 1) maintains continuity in position as well as direction of flow with the last shock added to the group, and 2) has finite speed. Otherwise, a new first-order shock branch should be initiated.
A2. A second-order shock hypothesis should be discarded if it is not initial, or if it does not subsequently give rise to two outward flowing first-order shock branches. Otherwise it should be kept and identified as the parent of the two first-order shock branches.
A3. A single first-order shock branch that intersects a third-order branch, or that terminates or emanates from a third-order shock branch's endpoints without maintaining continuity in orientation, should be discarded.
A4. Two third-order shock hypotheses should be grouped together if they are neighbors, and if their orientations are consistent (the shock group has to be smooth). Distinct groups of third-order shocks should not intersect, and any third-order shock that remains isolated should be interpreted as a fourth-order shock.
A5. A fourth-order shock hypothesis that is not isolated from other second-, third-, or fourth-order hypotheses should be discarded. A fourth-order shock that is isolated should be interpreted as a circle, otherwise it should be identified as the point of annihilation of the merging first-order branches.

Figure 10: Actions **A1-A5** are used to prune impossible shock configurations and organize surviving shocks.

dumbbell shape, leading to its description as two "seed-based" parts (fourth-order shocks) connected at a "neck" (second-order shock), with each part having three protrusions (first-order shock branches). Figure 12 illustrates the robustness of shock detection under rotation and stretching: the structural description of each triangle as a "seed with three protrusions merging onto it" and of each rectangle as a "bend with two protrusions at each end", is preserved. Next, the description of the shape in Figure 13 (top) as a hierarchical collection of protrusions converging onto a single seed is intuitive and can be used for recognition. The representation of the tool in Figure 13 (bottom) is suited to recognition: a different pair of pliers would match the structural description of "two large bends, attached at one end" (the handles) connected to "two smaller protrusions, attached at the other end" (the head); the same pair of pliers would have to match relative shock locations, formation times and velocities as well. Figure 14 illustrates the robustness of the representation in the face of occlusion, movement, and bending of parts: regions remote to the deformations are not affected and a qualitative description as a collection of bends attached to a hierarchy of protrusions emerges throughout. Finally, Figure 15 depicts the shock-based description of two handwritten letters (left) and the computation of shock speed and acceleration (right). In all the examples the shock branches are smooth and the representation allows for precise reconstruction and accurate metric measurements, as well as for qualitative perceptual shape classes. The latter are crucial for the identification of two different shapes as instances of the same category.

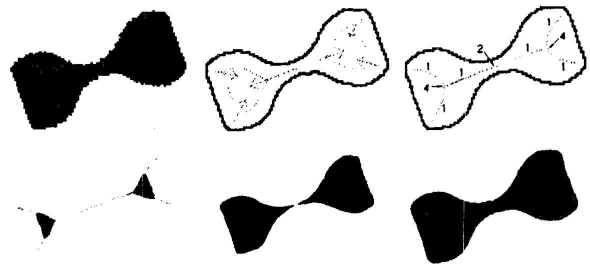

Figure 11: TOP: The evolution of shocks under inward reaction for a rotated dumbbell shape; the arrows depict the velocity of the last shock added to each branch. BOTTOM: The growth of the dumbbell from its shock-based description.

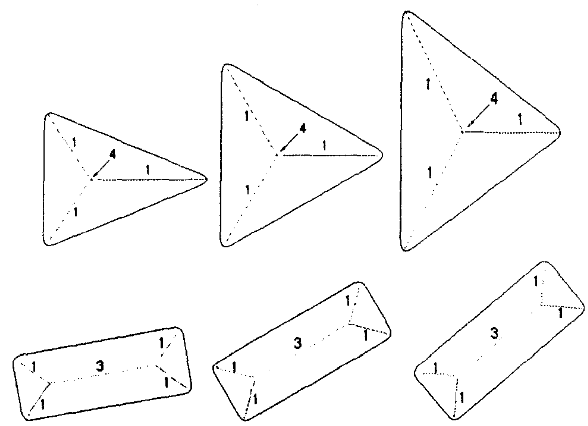

Figure 12: The shock branches remain smooth and no spurious branches are added under rotation or stretching. Further, the structural description of each triangle as "three protrusions converging onto a single seed" and of each rectangle as a "bend with two protrusions at each end" is preserved.

5 Structural Diffusion

A variety of approaches have been proposed to deal with the sensitivity of the SAT to boundary details, *e.g.*, blurring to create a multiresolution SAT [19], the use of residual functions [16], and non-linear diffusion of the shape's angle function [18]. Following the theoretical development of [8], the approach we suggest is to use curvature deformation (β_1) as a smoothing process to assign a significance to each shock group[6]:

Remark 1 (Significance) *The significance of a shock group is proportional to its survival with increasing amounts of curvature deformation.*

[6]This choice enforces a number of desirable properties, *e.g.*, in the case of $\beta_1/\beta_0 \rightarrow \infty$, any embedded curve will evolve to a round point without developing self-intersections or singularities [5], and the number of extrema and inflection points is non-increasing, implying that no new shock branches can form.

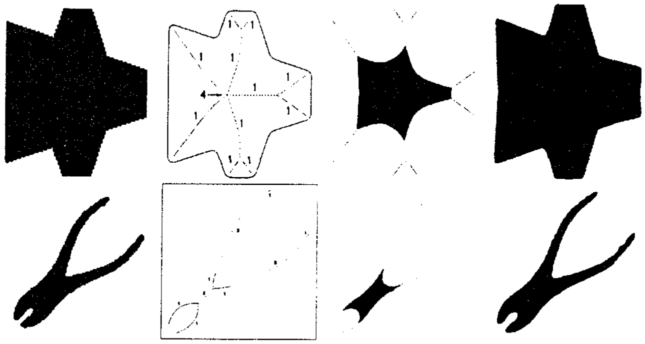

Figure 13: The shock-based description and growth of a shape composed of trapezoids (TOP), and of an industrial shape (BOTTOM). The originals shapes are on the left, and the reconstructions on the right.

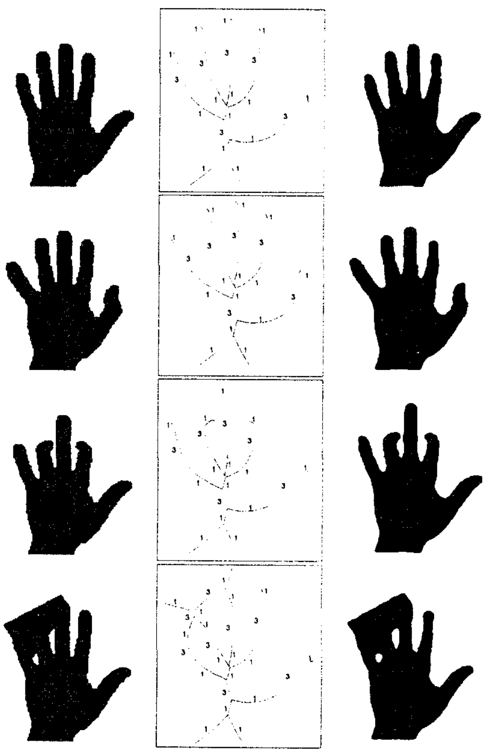

Figure 14: Shock detection under occlusion, and movement/bending of parts. LEFT: The original shapes. MIDDLE: The shock-based description. RIGHT: The reconstruction from shocks.

We consider the effect of diffusion on each shock type; the detection of shocks with diffusion is coarse (not subpixel), and *is only intended to provide a measure of significance for shocks obtained under pure reaction.* When $\beta_1 \neq 0$ we interpret a first-order shock as a maxima of (sufficiently high) positive curvature. The survival of a first-order shock group with increasing diffusion reflects the "scale" of the corresponding protrusion, Figure 16 [7]; the survival of a second-order shock with diffusion reflects how narrow the corresponding neck is, Figure 17; diffusion regularizes bend-like shapes with boundary perturbations [23]; and the survival of a fourth-order shock with diffusion reflects the degree to which it represents a local center of mass for a shape, *e.g.*, compare the rightmost and leftmost fourth-order shocks in Figure 17.

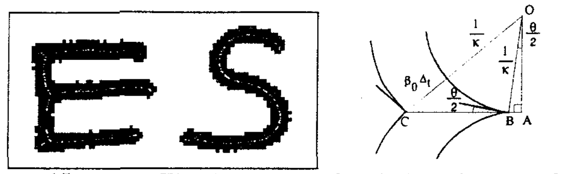

Figure 15: LEFT: The shock-based description of two handwritten letters. RIGHT: First-order shock speed and acceleration. The shock occurs at point B, and after one time step has moved to point C. With $AB = \kappa^{-1}sin(\theta/2)$, the speed of the shock is obtained as: $s = AB' = \beta_0/sin(\theta/2)$. The **acceleration** is obtained by differentiating the speed as: $a = s(\beta_0^2 - s^2)\kappa/\beta_0$.

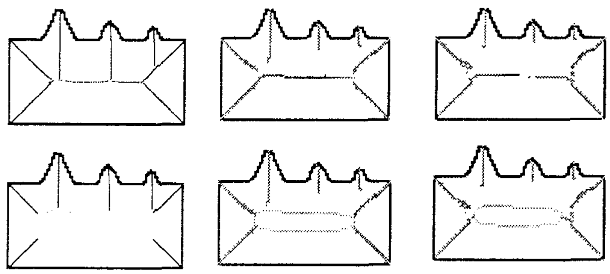

Figure 16: LEFT TO RIGHT: $\beta_0 = -0.2$, $\beta_1 = 0.0, 0.25, 0.5$. Each column depicts the shock groups that have been detected up until the present time, with the evolved shape overlaid. Observe that branches are annihilated in order of the scale of the protrusion they represent.

The above notion of significance induces a hierarchical ordering of shock branches from fine to coarse, *i.e.*, branches obtained under pure reaction are removed in the order that they annihilate under diffusion, and the structures that they represent are literally broken off, Figure 16. This brings out the coarse level similarity between shapes belonging to the same category, Figure 19, an essential requirement for recognition.

6 Shocks from Images

In conclusion, we suggest that the shock-based representation can be extended to apply to fragmented shapes as they typically arise in real imagery by allowing local edge hypotheses to interact via the evolution of a local embedding surface; recall that any Lipshitz continuous surface can be used. Such a surface can be constructed using the output of an edge operator, *i.e.*, by first placing oriented receptive fields at each edge, Figure 20 (top),

[7] In analogy to the lifetime of a grey-level blob in scale space [15], when two protrusions are nearby the shock branches may merge.

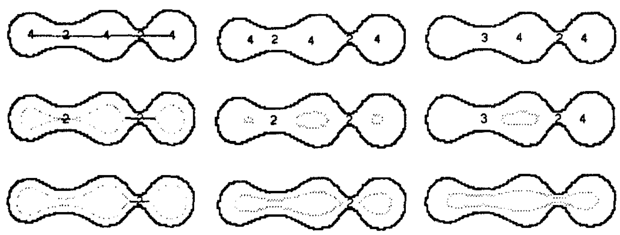

Figure 17: LEFT TO RIGHT: $\beta_0 = -0.2$, $\beta_1 = 0.0, 1.0, 1.5$. Each column depicts shocks that have been detected up until the present time, with the evolved shape overlayed; for $\beta_1 \neq 0$ we focus on the higher-order shocks: of the two necks, the weaker one on the left is the first to annihilate with increased diffusion.

Figure 18: The significance hierarchy induced by the computation in Figure 16; in the reconstructions protrusion branches have been removed in the order that they are annihilated with increased diffusion.

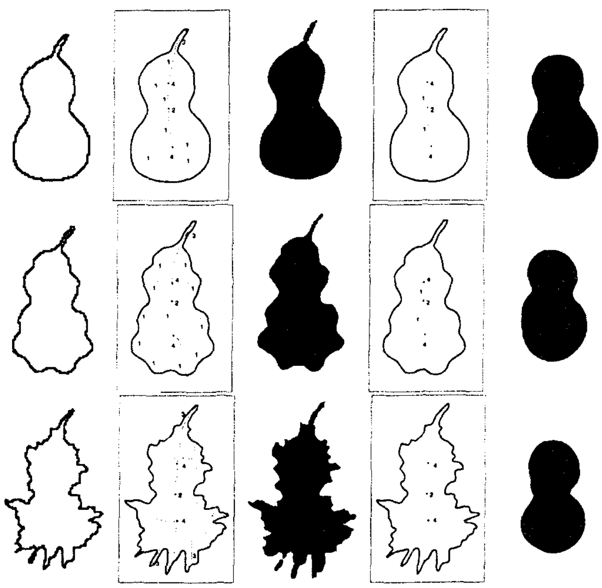

Figure 19: COLUMN ONE: The original pear shapes, taken from [20]. COLUMN TWO: The shock-based description under pure reaction. COLUMN THREE: The reconstruction based on the pure reaction description (column two). COLUMN FOUR: Those branches of the pure reaction description (column two) that survive under diffusion. COLUMN FIVE: The reconstruction based on the description in the fourth column brings out the coarse level similarity between the shapes.

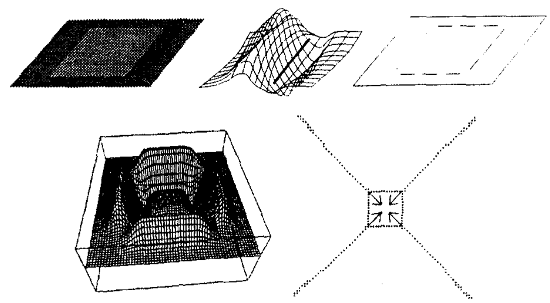

Figure 20: Shocks are obtained from a grey level image by placing oriented receptive fields at edge operator outputs to construct a covering surface (BOTTOM LEFT), and then applying shock detection to the evolving surface (BOTTOM RIGHT).

and then taking the union of all such receptive fields, Figure 20 (bottom left). By construction, the covering surface has the property that its zero-crossings pass through the original edge locations. Therefore, the evolution of the covering surface can allow for the detection, classification and grouping of shocks *prior* to obtaining a segmentation of the shape itself, Figure 20 (bottom right).

Acknowledgements The support of NSERC, and NSF grant IRI-9305630, is gratefully acknowledged. We thank Jonas August, Michael Kelly, Eric Pauwels, and Steve Zucker for helpful discussions.

References

[1] H. Blum. Biological shape and visual science. *J. Theor. Biol.*, 38:205–287, 1973.

[2] C. A. Burbeck and S. M. Pizer. Object representation by cores: Identifying and representing primitive spatial regions. *Vision Research*, 35:1917–1930, 1995.

[3] L. C. Evans and J. Spruck. Motion of level sets by mean curvature I. *J Differential Geometry*, 33(3):635–681, May 1991.

[4] P. J. Giblin and S. A. Brassett. Local symmetry of plane curves. *American Mathematical Monthly*, 92:689–707, December 1985.

[5] M. A. Grayson. The heat equation shrinks embedded plane curves to round points. *J. Differential Geometry*, 26:285–314, 1987.

[6] A. Harten, B. Engquist, and R. Sukumar. Uniformly high order accurate essentially non-oscillatory schemes, III. *J Comp. Physics*, 71:231–303, 1987.

[7] M. Kelly and M. D. Levine. Annular symmetry operators: A method for locating and describing objects. In *Fifth ICCV*, 1016–1021, Boston, June 1995.

[8] B. B. Kimia, A. R. Tannenbaum, and S. W. Zucker. Toward a computational theory of shape: An overview. In *First ECCV*, Antibes, France, 1990.

[9] —. The shape triangle: Parts, protrusions, and bends. In *Proceedings of the Int. Workshop on Visual Form*, pages 307–323, Capri, Italy, May 1994.

[10] —. Shapes, shocks, and deformations, I: The components of shape and the reaction-diffusion space. *Int. Journal of Computer Vision*, 15:189–224, 1995.

[11] P. D. Lax. *Shock Waves and Entropy*, pages 603–634. Academic Press, New York, 1971.

[12] H. Lewis and C. Papadimitriou. *Elements of the Theory of Computation*. Prentice-Hall, 1981.

[13] F. Leymarie and M. D. Levine. Simulating the grassfire transform using an active contour model. *IEEE PAMI*, 14(1):56–75, January 1992.

[14] M. Leyton. A process grammar for shape. *Artificial Intelligence*, 34:213–247, 1988.

[15] T. Lindeberg. *Scale-Space Theory In Computer Vision*. Kluwer, 1994.

[16] R. L. Ogniewicz. *Discrete Voronoi Skeletons*. Hartung-Gorre, 1993.

[17] S. Osher and J. Sethian. Fronts propagating with curvature dependent speed: Algorithms based on Hamilton-Jacobi formulations. *J Comp. Physics*, 79:12–49, 1988.

[18] E. J. Pauwels, P. Fiddelaers, and L. J. V. Gool. Enhancement of planar shape through optimization of functionals for curves. *IEEE PAMI*, (17):1101–1105, November 1995.

[19] S. M. Pizer, W. R. Oliver, and S. H. Bloomberg. Hierarchical shape description via the multiresolution symmetric axis transform. *IEEE PAMI*, 9(4):505–511, 1987.

[20] W. Richards, B. Dawson, and D. Whittington. Encoding contour shape by curvature extrema. *J. Optical Society of America*, 3(9):1483–1489, 1986.

[21] G. L. Scott, S. Turner, and A. Zisserman. Using a mixed wave/diffusion process to elicit the symmetry set. *Image and Vision Computing*, 7(1):63–70, February 1989.

[22] J. Serra, editor. *Image Analysis and Mathematical Morpholpogy, Part II: Theoretical Advances*. Academic Press, 1988.

[23] K. Siddiqi and B. B. Kimia. A shock grammar for recognition. Technical Report LEMS 143, LEMS, Brown University, September 1995.

[24] K. Siddiqi, B. B. Kimia, and C. Shu. Geometric shock-capturing eno schemes for subpixel interpolation, computation and curve evolution. In *International Symposium on Computer Vision*, Coral Gables, Florida, November 1995.